Hindawi
Journal of Chemistry
Volume 2019, Article ID 1768351, 12 pages
https://doi.org/10.1155/2019/1768351

Research Article

Conversion of Organic Matter in Coal by Photocatalytic Oxidation with H_2O_2 over SFC/TiO_2 in Isolated Oxygen System

Heng-Shen Xie,[1,2] **Zhi-Min Zong**,[2] **Yu-Gao Wang**,[2] **Pei-Zhi Zhao**,[2] **Shi-Hua Zhang**,[2] **Jun-Qiang Wang**,[1] **Hong Fu**,[1] **Shuang-Hua Liang**,[1] **Ling Su**,[1] **and Xian-Yong Wei**[2]

[1]*Jiangsu Engineering Laboratory of Biomass Resources Comprehensive Utilization, Jiangsu Vocational Institute of Architectural Technology, Xuzhou 221116, Jiangsu, China*
[2]*Key Laboratory of Coal Processing and Efficient Utilization (Ministry of Education), China University of Mining and Technology, Xuzhou 221008, Jiangsu, China*

Correspondence should be addressed to Heng-Shen Xie; hkxie_xz@163.com

Received 31 March 2019; Accepted 18 June 2019; Published 24 October 2019

Academic Editor: Sedat Yurdakal

Shenfu bituminous coal (SFBC), Geting coal (GTC), Shengli lignite (SLL), and Holingola coal (HLGLC) were oxidized by UV light radiation with aqueous H_2O_2 over SFC/TiO_2 in a closed suspension system (CSS) to understand structural characteristics of 4 typical Chinese coals. Raw and oxidized coals were dried and extracted with acetone thoroughly to ensure residue extraction. Meanwhile, the extracts were analyzed using a gas chromatograph/mass spectrometer. The results show that organic matters (OMs) in coals can be converted into a large number of oxygen-containing organic compounds (OCOCs), mainly containing ketones, esters, alcohols, etc. Oxidizing species such as hydroxyls, hydroperoxyl, and alkyl radicals are excited by light irradiation and substitute for hydrogen atoms of methyls and methylenes of acenes or branched-chain alkanes in coals. Acetic acid and acetaldehyde can be formed and dissolved in aqueous solution in the oxidation reaction. The yields can be improved with the enhancement of the oxidation effect.

1. Introduction

In understanding the composition and structure of organic matters (OMs) in coals and in using coals effectively, the mild oxidation and the separable and nondestructive analysis method of coals at the molecular level coals have increasingly been the focus of scientific study over the past decades [1–13]. Meanwhile, the oxidation products of coals are usually viewed as an important source of high value-added products [14–19]. However, the existing oxidation methods are less satisfactory due to their high dosages, high costs, and harsh conditions. Photocatalytic oxidation (PCO), as one of the advanced oxidation processes, has attracted extensive attention since 1972 [20–27] because of its low temperature, high efficiency, and low selectivity. In recent years, the PCO of coals including solid-gas mixed systems (UV/O_2/TiO_2) and solid-gas-liquid heterogeneous systems (H_2O/UV/air/TiO_2) has received considerable attention [28–30]. Nevertheless, the component analysis of oxidized coals is often complicated by many kinds of oxidizing particles detected in the systems. Especially, previous studies have found that oxygen molecules can be stimulated by light to generate singlet or triplet oxygen, the main oxidizing substances, which can enhance the oxidation of OMs in coal and inhibit the recombination of electron hole and pairs due to the existence of the photoelectron capture center [31–33]. Meanwhile, the oxygen-related oxidation may increase the complexity of products and thus make the mechanism analysis of coal oxidation more difficult

[34–37]. Hence, an isolated oxygen system was designed to oxidize four species coals, and results were analyzed by using gas chromatograph/mass spectrometer (GC/MS). In the system, the inducted OMs conversion rule proved that it is completely possible to realize coal mild oxidation effectively and utilize coal efficiently by controlling the species and quantities of reactants. In addition, the Fourier transform infrared spectroscopy analysis of coal PCO is scarcely noted in the literature.

2. Experiment

2.1. Samples and Reagents. Shenfu bituminous coal (SFBC), Geting coal (GTC), Shengli lignite (SLL), and Holingola coal (HLGLC) were, respectively, collected from Shaanxi Province, Shandong Province, Shaanxi Province, and Inner Mongolia Autonomous Region. Placed in a desiccator, all coals were pulverized to pass through a standard sieve of 0.074 mm. Their proximate and ultimate analyses are shown in Table 1. Purchased as commercially available, analytical reagents acetone and ether were distilled in a Büchi R-134 rotary evaporator prior to use. The catalyst (SFC/TiO_2) was a man-made nanometer powder [32]. The mass percentage of the commercially purchased H_2O_2 was 30%.

2.2. Experimental Methods and Procedures. As shown in Figure 1, dried coal (2 g) was mixed with the catalyst (0.01 g), and H_2O_2 (30 ml) was added dropwise to the 100 ml quartz tube to obtain a reaction mixture system. After 10 minutes of low-power ultrasonic dispersion, the mixture was illuminated with a 500 W low-pressure UV mercury lamp for 4 hours under magnetic stirring. Thereafter, the mixture was filtered in a sand core funnel in vacuum. Filtrate portions (FPs) were extracted exhaustively with ether to separate ether-soluble fractions (ESFs) and ether-insoluble fractions (EIFs). EIFs were extracted with acetone to gain acetone-soluble fraction (ASFIs). The weight of acetone-soluble fraction (WASFI) can be obtained by ASFIs volatile naturally. Filter cakes (FCs) were dried in vacuum at 50°C to 60°C for 2 hours to obtain drying filter cakes (DFCs) and weighted to get weight acetone-soluble fraction (WASFII). FCs were dispersed by using carbon disulfide for 2 minutes and extracted exhaustively with 200 ml acetone to obtain acetone-soluble fractions (ASFIIs). ESFs and ASFs were concentrated through rotary evaporation and analyzed with GC/MS. The extract yields (EYs) were marked as EY, EY_I, EY_{II}, EY_{III}, and EY_{IV} corresponding to the blank sample and different oxidation systems.

The experiment was completed through four systems, in which the same amount of H_2O_2 and coal but different amounts of catalyst were employed during different illumination hours. In the first oxidation system, 0.1 g of catalysts were used during 4 hours of irradiation to get the extracts of oxidized coals, marked, respectively, as ASF_{OSFBCI}, ASF_{OGTCI}, ASF_{OSLLI}, and ASF_{OHLGLI}. In the second oxidation system, 0.1 g of catalysts were used during 12 hours of illumination to get the extracts, labeled as $ASF_{OSFBCII}$, ASF_{OGTCII}, ASF_{OSLLII}, and $ASF_{OHLGLCII}$. In the third oxidation system, 0.05 g of catalysts were used during 12 hours of irradiation to get the extracts, labeled as $ASF_{OSFBCIII}$, $ASF_{OGTCIII}$, $ASF_{OSLLIII}$, and $ASF_{OHLGLCIII}$. In the fourth oxidation system, no catalyst was used and 4 hours of reaction time brought forth the extracts, marked as $ASF_{OSFBCIV}$, ASF_{OGTCIV}, ASF_{OSLLIV}, and $ASF_{OHLGLCIV}$.

Table 1: Proximate and ultimate analyses (wt.%) of coals.

Coal	Proximate analysis			Ultimate analysis (daf)			$S_{t,d}$ (wt.%)
	M_{ad}	A_d	V_{daf}	C	H	N	
SFBC	10.21	6.50	37.70	80.51	4.82	0.90	0.40
GTC	8.51	5.71	35.00	82.95	5.47	1.13	1.00
SLL	20.07	11.35	46.77	38.99	2.78	0.19	1.00
HLGLC	17.31	23.45	43.42	42.35	2.68	0.43	0.57

daf: dry and ash-free base; M_{ad}: moisture (air-dried base); A_d: ash (dry base, i.e., moisture-free base); V_{daf}: volatile matter (dry and ash-free base); $S_{t,d}$: total sulfur (dry base).

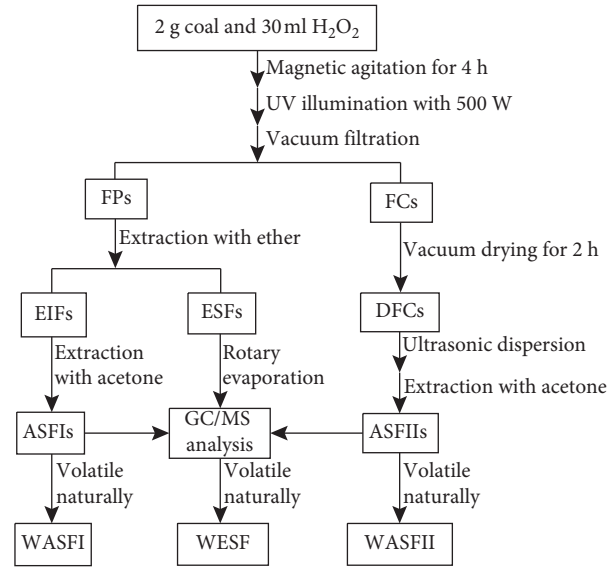

Figure 1: Procedure for coal oxidation in SSC.

2.3. GC/MS Analysis. GC/MS analysis was conducted with a Hewlett-Packard 6890/5973GC/MS, which was equipped with a capillary column coated with HP-5MS (cross-link 5% PH ME siloxane, 30 m × 0.25 mm i.d., and 0.25 μm film thickness) and a quadrupole analyzer in the electron impact mode at 70 eV. The injection and detector temperatures were set to 300°C. The column temperature was programmed to range from 100°C to 200°C at a rate of 15°C·min^{-1} for 5 minutes before being increased to 300°C at a rate of 8°C·min^{-1} for 15 minutes. Data were obtained and processed by the Chemstation software. The compounds were identified by comparing their mass spectra with the NIST05 library data. The residues were dried in vacuum for 10 hours and weighed to calculate the extraction yield by difference.

Table 2: Organic compounds detected in AEF_{SFBC}, AEF_{OSFBCI}, and $AEF_{OSFBCIV}$.

Peak	Parent compound	Detected in		
		ASF_{SFBC}	ASF_{OSFBCI}	$ASF_{OSFBCIV}$
	NAs			
60	Nonacosane	2.0		
64	Octacosane	2.0		
71	Heneicosane	3.2		
74	Tetracosane	5.6		
78	Heptadecane	3.0		
79	Tetratetracontane	1.8		2.1
80	Docosane	5.6		
82	Tritetracontane			2.9
84	Tetratriacontane	2.0		
	BA			
51	2,6,10,14-Tetramethyl-hexadecane	1.9		
	Branched cyclane			
41	9-Dodecyl-tetradecahydro-anthracene			1.8
	Alkenes			
20	1-Methyl-5,6-divinylcyclohex-1-ene		3.6	
26	4a,8,9,9-Tetramethyl-1,2,3,4,4a,5,6,8a-octahydro-1,4-methano-naphthalene	2.3		
44	1,2-Dimethyl-cyclohexene	2.1		
	CA			
58	Phthalic acid mono-(1-butyl-2-ethyl-hexyl) ester	6.8		
	Alkylarenes			
43	1,1,2,3,3-Pentamethyl-indane	2.7		
66	7-Butyl-1-hexyl-naphthalene	8.4		
76	7-Isopropyl-1-methyl-phenanthrene	11.0	1.2	
77	1-Propyl-4-(2-*p*-tolylethynyl)benzene	1.7		
81	8-Isopropyl-1,3-dimethyl-phenanthrene	1.4		
	Alkanols			
6	2-Methyl-hexan-2-ol		2.3	
7	Octan-3-ol			1.7
13	3-Isopropenyl-2-methyl-cyclohexanol		2.5	
16	Octanol		2.3	
32	2-Isopropenyl-5-methyl-cyclohexanol		1.4	
	Arenols			
19	2-*tert*-Butyl-4,6-dimethyl-phenol		2.0	
	Ketones			
1	Cyclohexanone		14.8	
9	2,6-Dimethyl-hepta-2,5-dien-4-one		44.6	50.2
11	3,5,5-Trimethyl-cyclohex-2-enone		2.7	
18	1-(4,7,7-Trimethyl-bicyclo[4.1.0]hept-3-en-3-yl)-ethanone		5.1	
28	4-(2,6,6-Trimethyl-cyclohex-1-enyl)-but-3-en-2-one	4.9		
59	2,4-Dimethyl-hexan-3-one			3.2
	Esters			
4	Acetic acid 1,2-dimethyl-propyl ester	9.0		
30	Acetic acid 17-(5-methoxy-1,5-dimethyl-4-oxo-hexyl)-4,4,13,14-tetramethyl-tetradecahydro-cyclopropa[9,10]cyclopenta[a]phenanthren-3-yl ester	2.1		
72	Methoxy-acetic acid 1-methyl-tridecyl ester			2.6
	NCOCs			
5	*N*-(5-Oxo-2,5-dihydro-furan-2-yl)-acetamide		1.3	
12	2,6-Dimethyl-6-nitro-hept-2-en-4-one	6.3	16.1	33.5
67	3-(2,4,6-Trimethyl-phenyl)-pyridine			2.0
68	7-Ethyl-2,4-dimethyl-10H-benzo[b][1,8] naphthyridin-5-one	4.5		
	CCOC			

Table 2: Continued.

Peak	Parent compound	Detected in		
		ASF_{SFBC}	ASF_{OSFBCI}	$ASF_{OSFBCIV}$
10	2-Chloro-4-isopropyl-1-methyl-benzene OCOC	1.2		
40	2,4,5,5,8a-Pentamethyl-6,7,8,8a-tetrahydro-5*H*-chromene	8.2		

3. Results and Discussion

3.1. GC/MS Analysis of Oxidized Coal

3.1.1. Effect Analysis of ASF_{SFBC} and ASF_{OSFBC}. SFBC and OSFBC were extracted with acetone and analyzed by GC/MS to understand OM hydrothermal conversion in coals in the process. Results show that no OMs were detected in $ASF_{OSFBCII}$ and $ASF_{OSFBCIII}$, except in ASF_{OSFBCI} and $ASF_{OSFBCIV}$, indicating that ASFs can be oxidized completely during 12 hours of illumination despite the decreasing amount of photocatalyst from 0.1 g to 0.05 g. Thus, only the analysis results of ASF_{OSFBCI} and $ASF_{OSFBCIV}$ are presented in Table 2. As listed in Table 2, the depolymerization of some part of the OMs is indicated by the result that 24 OMs were confirmed in ASF_{SFBC}, but only 13 OMs in ASF_{OSFBCI} and 9 OMs in $ASF_{OSFBCIV}$. Oxygen atoms were introduced in the process, according to the result that the relative content (RC) of 7-isopropyl-1-methylphenanthrene (peak 76) is the highest in ASF_{SFBC}, whereas the proportion of 2,6-dimethylhepta-2,5-dien-4-one is the highest in ASF_{OSFBCI} and $ASF_{OSFBCIV}$. According to the analysis, the oxygen atoms may have two sources: the compounds self-depolymerization in coal resulted from the cleavage of C–O and the oxidation of hydroxyl radicals. Among the 13 OMs in ASF_{OSFBCI}, 1 branched alkane (BA), 1 alkylarene, 1 arenol, 4 alkanols, 4 ketones, and 2 nitrogen-containing compounds (NCOCs) were detected. By contrast, in $ASF_{OSFBCIII}$, 2 NAs, 1 BA, 1 ketone, 1 NCOC, 1 alkanol, 1 ester, and 1 ketone were detected. Quantitative analysis verified that OMs have been converted partly in the process. Possible evidences are as follows: firstly, the RCs of NAs and the number of carbon atoms in long-chain alkanes decrease. 8 NAs in ASF_{SFBC} but no NA in ASF_{OSFBCI} and 2 NAs in $ASF_{OSFBCIV}$ were detected, and their RCs have been reduced from 25.20% to 5.00% before and after oxidation (as shown in Figure 2). It can be interpreted that almost all NAs have been converted successfully, and no more NAs may be formed despite the extension of illuminating time [31]. Secondly, the amount of branched-alkanes (BAs) in ASF_{OSFBCI} and $ASF_{OSFBCIV}$ decreases significantly compared with those in ASF_{SFBC}. As listed in Tables 2 and 3, BAs and 5 alkylarenes containing α-H atoms account for 31.50% in ASF_{SFBC} after oxidation, only 1 BA and 1 alkylarene in ASF_{OSFBCI} and 1 BA in $ASF_{OSFBCIV}$ are verified, and the RCs of the BAs and alkylarenes in ASF_{OSFBCI} and in $ASF_{OSFBCIV}$ decrease to 4.80% and 1.80%, respectively. These findings show that the majority of BAs or alkylarenes have been oxidized

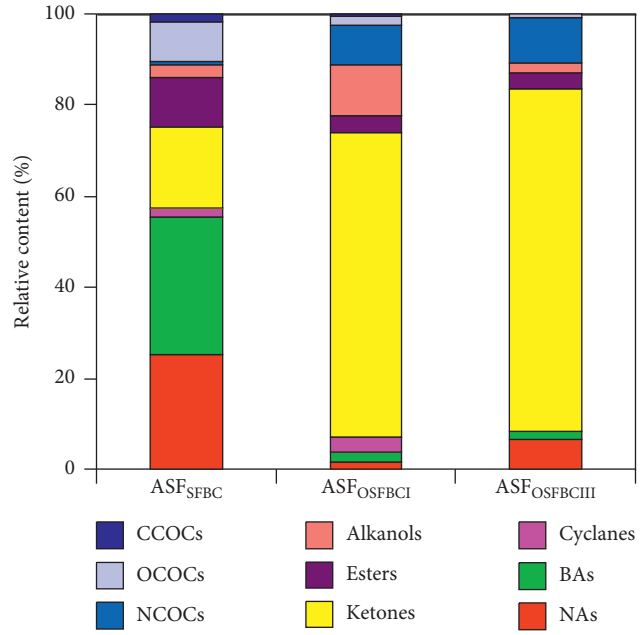

Figure 2: Component analysis of ASF_{SFBC}, ASF_{OSFBCI}, and $ASF_{OSFBCIV}$.

through α-H atoms substitution of photoelectron and photogenic-free radicals. Thirdly, there is no change in the number of oxygen-containing organic compounds (OCOCs) in ASF_{OSFBCI} and $ASF_{OSFBCIV}$ after the oxidation. However, their RCs increased significantly from 43.00% in ASF_{SFBC} to 92.80% in ASF_{OSFBCI} and 93.20% in $ASF_{OSFBCIV}$. More importantly, 2,6-dimethylhepta-2,5-dien-4-one is detected both in ASF_{OSFBCI} and in $ASF_{OSFBCIV}$, and theirs RCs are the highest (accounting for 44.60% and 50.20%, respectively), which indicate that the formation of ketones is the main process of photo-oxidation conversion.

According to the basic principle of photolysis, the excited electronic transition from valence band to conduction band on the surface of the photocatalyst causes the formation of electron hole pairs. The pairs bring about hydrogen peroxide and water cracking to produce hydroxyl radicals, which oxidize OMs in coal and form various free radicals. All radicals in the aqueous system react with OMs each other to obtain depolymerization products. Thus, the formation of alkanols, ketones, and esters should result in NA and BA oxidation conversion and can also lead to the dramatic reduction or diminishing of reactant quantity. The decreasing trend of alcohol conversion indicates that the oxidation susceptibility of the third oxidation system is

Table 3: Organic compounds detected in ASF_{GTC} and ASF_{OGTCI}.

Peak	Parent compound	Detected in	
		ASF_{GTC}	ASF_{OGTCI}
	NAs		
46	Heneicosane	2.9	
56	Heptadecane	3.9	1.9
57	Heptacosane	2.2	
59	Tetratriacontane	3.7	
	Bas		
29	2,6,10,14-Tetramethyl-pentadecane	2.9	
	Alkenes		
20	(3-Methyl-penta-1,2,4-trienyl)-benzene	1.6	
	Alkylarenes		
13	1-Methyl-naphthalene		2.2
16	2,3-Dimethyl-naphthalene		1.6
18	1,4-Dimethyl-naphthalene		3.1
19	2,6-Dimethyl-naphthalene	2.6	
22	2,3,6-Trimethyl-naphthalene	1.6	1.2
23	4,6,8-Trimethyl-azulene		2.3
25	1,6,7-Trimethyl-naphthalene	3.5	
26	1,5,7-Trimethyl-naphthalene		2.7
27	1,4,5-Trimethyl-naphthalene	5.6	
30	4-Isopropyl-1,6-dimethyl-naphthalene	8.5	3.0
34	7-Isopropyl-1-methyl-naphthalene		2.5
35	7-Ethyl-1,4-dimethyl-azulene	4.2	
44	2-Methyl-anthracene	7.3	
52	2-Methyl-octadecane	2.6	
54	1-Methyl-pyrene		1.5
55	2-Methyl-fluoranthene	2.7	
	NSAs		
43	Naphtho[2,3-b]norbornadiene		1.3
49	Pyrene	1.9	
51	Fluoranthene	6.3	2.4
	Esters		
1	3-Methyl-*5H*-furan-2-one		20.7
9	Acetic acid *m*-tolyl ester		1.8
10	Acetic acid *p*-tolyl ester		1.3
12	Acetic acid 2,3-dimethyl-phenyl ester		3.6
32	Acetic acid 3,4-diacetoxy-6,8-dioxa-bicyclo[3.2.1] oct-2-yl ester		3.9
60	Phthalic acid 1-(2,2-dimethyl-propyl)ester 2-(2-ethyl-hexyl) ester		1.1
	Ketones		
2	Hexane-2,5-dione		18.3
4	2-Methylcyclopent-2-enone		1.3
6	2,6-Dimethyl-hepta-2,5-dien-4-one	7.0	8.7
7	3,5,5-Trimethyl-cyclohex-2-enone		3.5
15	1-(3,5,5-Trimethyl-cyclohex-2-enylidene)-propan-2-one		3.5
40	(2,4-Dimethyl-phenyl)-phenyl-methanone	1.4	
	NCOC		
8	2,6-Dimethyl-6-nitro-hept-2-en-4-one	24.9	3.5
	Alkanols		
5	4-Methyl-heptan-3-ol	1.4	
11	Octan-3-ol		3.3
	Arenol		
41	4-Cyclohexyl-benzene-1,3-diol	1.4	

greater than that of the first system. Therefore, the reaction process must be optimized to obtain a desirable result.

In addition, many chromophores including the conjugated double bond and heterocyclic groups with nitrogen, sulfur, phosphorus, and chloride as bridged bonds were considered as important factors in determining the color of the compound and were excited easily by UV irradiation. Therefore, the photocatalytic decomposition of heteroatomic-

containing compounds (HCCs) in coal is most likely to occur. As listed in Table 2, 2,6-dimethyl-6-nitro-hept-2-en-4-one was detected in ASF_{OSFBCI} and $ASF_{OSFBCIV}$, accounting for 16.10% and 33.50%, respectively, but only 6.30% in ASF_{SFBC}, indicating that macromolecular heteroatom compounds in coals have been excited by light through chemical bond fracture between carbon atom and heteroatom firstly. 2,4,5,5,8a-Pentamethyl-6,7,8,8a-tetrahydro-5*H*-chromene and 1,2-dimethyl cyclohex-1-ene can be excited only in ASF_{SFBC}, whereas 1-methyl-5,6-divinylcyclohex-1-ene was confirmed in ASF_{OSFBCI} (ca. 3.60%), indicating that photo-oxidation depolymerization must have occurred in the process of photolysis. It has proven that the branched hydrocarbons can be converted preferentially and the polycyclic aromatic compounds can be depolymerized and converted into other small molecule compounds. And it is a proof of ring opening or cleavage link, suggesting that chromophore groups are favorable for photoelectron delivery and light energy utilization.

3.1.2. Effect Analysis of ASF_{GTC} and ASF_{OGTC}. OMs in SFBC could be converted into OCOCs under CSS as the upper experiment. GTCs were oxidized in the similar condition as the oxidation of SFBC to verify the coal oxidation laws and to understand the composition and structure of coals distributed in different regions. The results were analyzed by GC/MS and listed in Table 3. No OM was detected in ASF_{OGTCII}, $ASF_{OGTCIII}$, and ASF_{OGTCIV}, except in ASF_{OGTCI}, which indicates that OMs in GTC are more difficult to obtain than those in SFBC and the oxidation systems exhibit different properties.

Table 3 lists 22 OMs, including 4 NAs, 9 alkylarenes, 2 ketones, 2 NSAs, 1 NCOC, 1 BA, 1 alkanol, 1 arenoland, and 1 alkene in ASF_{GTC}. Among them, the abundance of 2,6-dimethyl-6-nitrohept-2-en-4-one is the highest. However, 25 OMs, including 1 NA, 9 alkylarenes, 2 NSAs, and 13 OCOCs, were detected in ASF_{OGTCI}, and their RCs are consecutively 1.9%, 20.1%, 3.7%, and 74.5% (as shown in Figure 3). Notably, in comparison with those in ASF_{GTC}, OCOCs in ASF_{OGTCI} increase but NAs and BAs decrease. The OMs in GTC have been oxidized successfully because of the active hydrogen atoms replaced by radicals. Nonetheless, the oxidation degree is different from that of SFBC because of the difference between the species and the quantity of OCOCs detected in ASF_{OGTCI} and in ASF_{OSFBCI}. Most probably, the coals have different structures and compositions resulting from different geographical positions and formation mechanisms. The experimental data also verified that GTC is more difficult to be oxidized by UV irradiation compared with SFBC. It is proved that GTC, which is formed in high humidity marine climate environment, has a more dense structure and fine compositions as a result of its high coalification degree.

3.1.3. Effect Analysis of ASF_{SLL}, ASF_{OSLLI}, and ASF_{OSLLIV}. SLL is generally considered to be oxidizable in mild conditions. It was oxidized under the same conditions as those

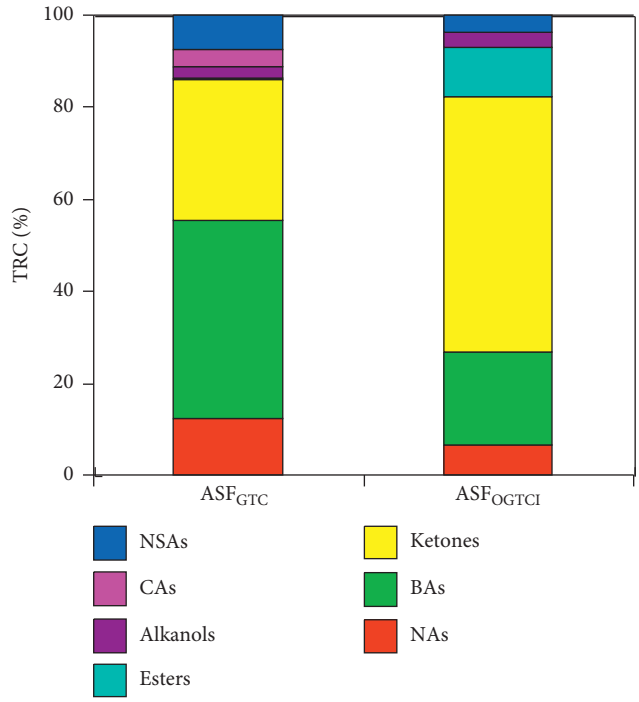

Figure 3: Component analysis of ASF_{GTC} and ASF_{OGTCI}.

of the upper two coals. The results are listed in Table 4. No peaks were detected in ASF_{OSLLII} and $ASF_{OSLLIII}$.

As shown in Table 4, 25 OMs in total were detected in ASF_{SLL}, ASF_{OSLLI}, and ASF_{OSLLIV}. 2,6-Dimethyl-6-nitro-2-hepten-4-one was confirmed in the three samples simultaneously and contained the maximum amount of OMs in ASF_{SLL}. Yet, 2,6-dimethyl-hepta-2,5-dien-4-one, the highest content compound in the two oxidation coals, was merely detected in ASF_{OSLLI} and ASF_{OSLLIV}, and their proportions are 49.9% and 58.8%, respectively. It indicates that 2,6-dimethyl-hepta-2,5-dien-4-one is the major conversion product in oxidation SLL and its formation mechanism should be heteroatom detachment because of the breaking of C-N bonds as in Scheme 1. In addition, the confirmation of only four OMs in ASF_{OSLLI} and three OMs in ASF_{OSLLIV} indicates that a large number of OMs in SLL have been oxidized and converted into OCOCs. Compared with SFBC and GTC, large numbers of heterogeneous compounds (containing N, P, and O), as photosensitive substances, were detected in ASF_{SLL} and degraded largely in ASF_{OSLLI} and ASF_{OSLLIV}. Analysis results also proved that SLL is a type of lignite with relatively low coalification degree and high activity. Given that only H_2O_2 takes part in the closed system, the oxidation of SLL and the formation of OCOCs should also have active hydrogen substituted by hydroxyl radicals rather than oxygen atoms or other oxidizing ions. Certainly electrophilic reaction is also the main process in the oxidation of SLL.

3.1.4. Effect Analysis of ASF_{HLGLC} and $ASF_{OHLGLCI}$. HLGLC, a typical lignite distributing in Northern China, was oxidized in the same condition as that of the upper coals. The results showed that no peaks were observed in the total ion chromatograms of $ASF_{OHLGLCII}$, $ASF_{OHLGCLCIII}$, and

Table 4: Organic compounds detected in ASF_{SLL}, ASF_{OSLLI}, and ASF_{OSLLIV}.

Peak	Parent compound	Detected in		
		ASF_{SLL}	ASF_{OSLLI}	ASF_{OSLLIV}
	NA			
32	Tetratetracontane	5.1		
	Bas			
17	4-Methyl-octane	2.0		
30	2,3,8-Trimethyl-decane	4.9		
	NCOCs			
1	3-Methyl-3-nitro-butyric acid ethyl ester	1.8		
2	Pyrrolidin-3-ol	1.4		
3	(1*Z*)-1-((*E*)-Pent-3-en-2-ylidene)semicarbazide		9.3	
7	2,6-Dimethyl-6-nitro-hept-2-en-4-one	34.4	39.4	32.4
8	4,6-Dimethyl-pyrimidin-2-ylamine	2.4		
	Esters			
4	Oxalic acid cyclohexyl ester hexyl ester			8.9
23	Phthalic acid diisobutyl ester	9.2		
26	7-Isopropenyl-3,6-dimethyl-6-vinyl-hexahydro-benzofuran-2-one	2.8		
	Alkanols			
5	Octan-3-ol		1.4	
12	(2-Hydroxymethyl-cyclohexyl)methanol	2.4		
	Ketones			
6	2,6-Dimethyl-hepta-2,5-dien-4-one		49.9	58.8
21	6,10-Dimethylundec-9-en-2-one	2.7		
29	Crinan-1-one	1.5		
	OCOC			
10	2,2,4-Trimethyl-oxetane	5.2		
	Cas			
15	4-Methyl-2-oxo-pentanoic acid	3.4		
25	Phthalic acid mono-(1-methyl-pentyl)ester	1.5		
33	Phthalic acid mono-[3-ethyl-1-(3-methyl-butyl)-heptyl]ester	2.8		
	NSA			
22	Anthracene	7.6		
	Alkylarenes			
24	Diphenyl-penta-1,3-diene	2.6		
28	Hexa-1,3-dienyl-benzene	2.3		
31	7-Isopropyl-1-methyl-phenanthrene	2.1		
	Branched cyclane			
34	17-(1,5-Dimethyl-hexyl)-10,13-dimethyl-2,3,4,5,6,7,8,9,10,11,12,13,16,17-tetradecahydro-1*H*-cyclopenta[*a*]phenanthrene	1.8		

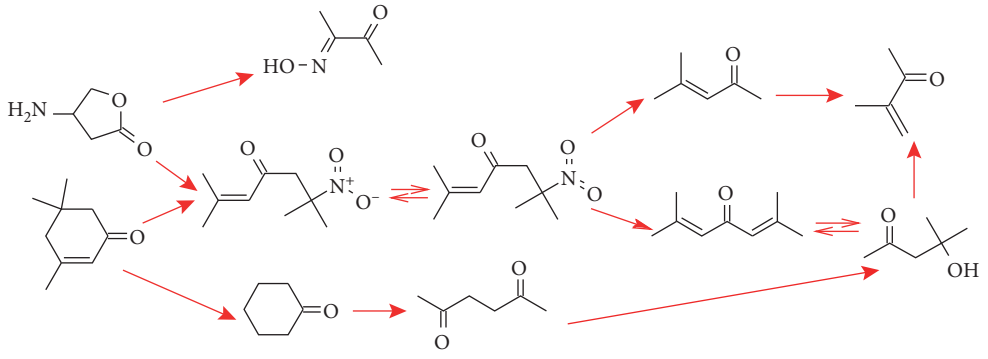

Scheme 1: Possible pathways of oxidation product formation in coals in PCO.

$ASF_{OHLGLCIV}$, except for those of ASF_{HLGLC} and $ASF_{OHLGLCI}$. Thus, only the analysis data of ASF_{HLGLC} and $ASF_{OHLGLCI}$ are listed in Table 5.

As shown in Table 5, seven OMs were detected in ASF_{HLGLC}, but only three OMs were detected in $ASF_{OHLGLCI}$. Notably, 2,6-dimethyl-6-nitro-hept-2-en-4-

Table 5: Organic compounds detected in ASF_{HLGLC} and $ASF_{OHLGLCI}$.

Peak	Parent compound	Detected in	
		ASF_{HLGLC}	$ASF_{OHLGLCI}$
	NCOCs		
1	Pent-3-en-2-ylidene-semicarbazide		27.2
6	2,6-Dimethyl-pyridin-3-ol		54.3
7	2,6-Dimethyl-6-nitro-hept-2-en-4-one	62.7	18.5
	OCOCs		
4	1-(1-Methoxy-ethoxy)-hex-3-ene	2.1	
	Ketones		
5	2,6-Dimethyl-hepta-2,5-dien-4-one	18.8	
12	Bicyclohexyl-2′-en-2-one	1.4	
	Alkanol		
8	Octan-3-ol	8.5	
	Esters		
9	Acetic acid 3-methyl-1-methylene-but-2-enyl ester	1.1	
13	Phthalic acid diethyl ester	1.4	

one exists both in ASF_{HLGLC} and $ASF_{OHLGLCI}$, but its amount decreases from 62.7% to 18.5% before and after oxidation. As a result of the fracture of the carbon nitrogen bond and the introduction of oxygen atoms by hydroxyl substituting, OCOCs have become the compounds with the highest abundance. Pent-3-en-2-ylidene-semicarbazide accounts for 27.2% in $ASF_{OHLGLCI}$, indicating that more NCOCs tend to be converted into the compound containing the peptide bond through ring opening and restructuring. From the previous analysis, HLGLC is more easily oxidized than SFBC and GTC. Although OCOCs are also the species with the highest abundance in HLGLC and SLL, the number of their species decreases in OHLGLC and OSLL, indicating that two coals were formed in oxygen-abundant regions or evolved from oxygen-rich substances.

In addition, the color of the extract differs because of the variation in the oxidation degree. In turn, the extract colors of ASF_{GTC}, ASF_{SFBC}, ASF_{SLL}, and ASF_{HLGLC} deepened consecutively to yellow to red to rufous. Those of their oxidized coals present the same tendency, indicating that a large number of photosensitive materials exist in lignite and can be oxidized through degradation and decolorization in PCO.

3.2. Analysis of ESFs in Oxidized Coals. As FPs were extracted with ether rapidly and exhaustively, ESFs were collected and analyzed by GC/MS. The results are shown in Figure 4. EIFs were analyzed with the UV-visible spectrum, and two peaks (with wavelengths of 220 and 275 nm) were detected. Their intensities were stronger than those of the blank sample. The aqueous solution is yellow, and the result of potassium permanganate titration is less than that of deionized water. Therefore, the aqueous solution may only contain inorganic salt.

As shown in Figure 4, carbon dioxide, acetic acids, and acetate can be confirmed in ESFs. Among them, acetate mainly contains Mg or Mn atoms and only exists in ESF_{OGTCI} and ESF_{OGTCII}, indicating that the oxidation efficiency is different from our coals for different compositions and structures. Meanwhile, the RC of carbon dioxide has the highest abundance among the three peaks of ESF_{OSFBCI}, ESF_{OGTCI}, ESF_{OSLLI}, and $ESF_{OHLGLCI}$, but acetic acid has the highest abundance in $ESF_{OSFBCII}$, ESF_{OSLLII}, and $ESF_{OHLGLCII}$, except in ESF_{OGTCII}. Carbon dioxide as a primary product exists in the weak oxidation system, but acetic acid is considered as an intermediate product in the stronger oxidation system. The data reveal that OMs in coals have been depolymerized, particularly OMs oxidized in an environment with strong polarity, although GTC is more difficult to oxidize than the other coals. Certainly, GTC has a stable structure and composition due to its distribution area and formation time. The exchange of oxocompounds is the main feature in coal oxidation even in CSS. Furthermore, the peak time of the reactant in OMs was postponed and the dispersibility of the resultants was improved. Most OMs in coals and oxidized coals were confirmed by GC/MS, and their conversion rules were deduced in Scheme 1.

3.3. Effect of EYs. EYs can indirectly explain the construction and composition of coals according to the quantity of OM conversion. Thus, the EYs of coals and oxidized coals were analyzed through the differential method. The results are shown in Figure 5.

As shown in Figure 5, the EYs of coals exhibit an increasing tendency with the optimization of the reaction condition. The EYs of SLL and HLGLC are higher than those of the other coals, indicating that lignite and bituminous coal were more oxidizable and more OMs were possibly converted into OCOCs in the oxidation system. The study has proven that SLL and HLGLC are composed of OMs with low coalification degrees. Due to the different formation periods and the geological formation environment of SFBC and GTC, the structure and composition of OMs in SFBC and GTC are different from those in SLL and HLGLC. The conversions are significantly different even in the same oxidation condition.

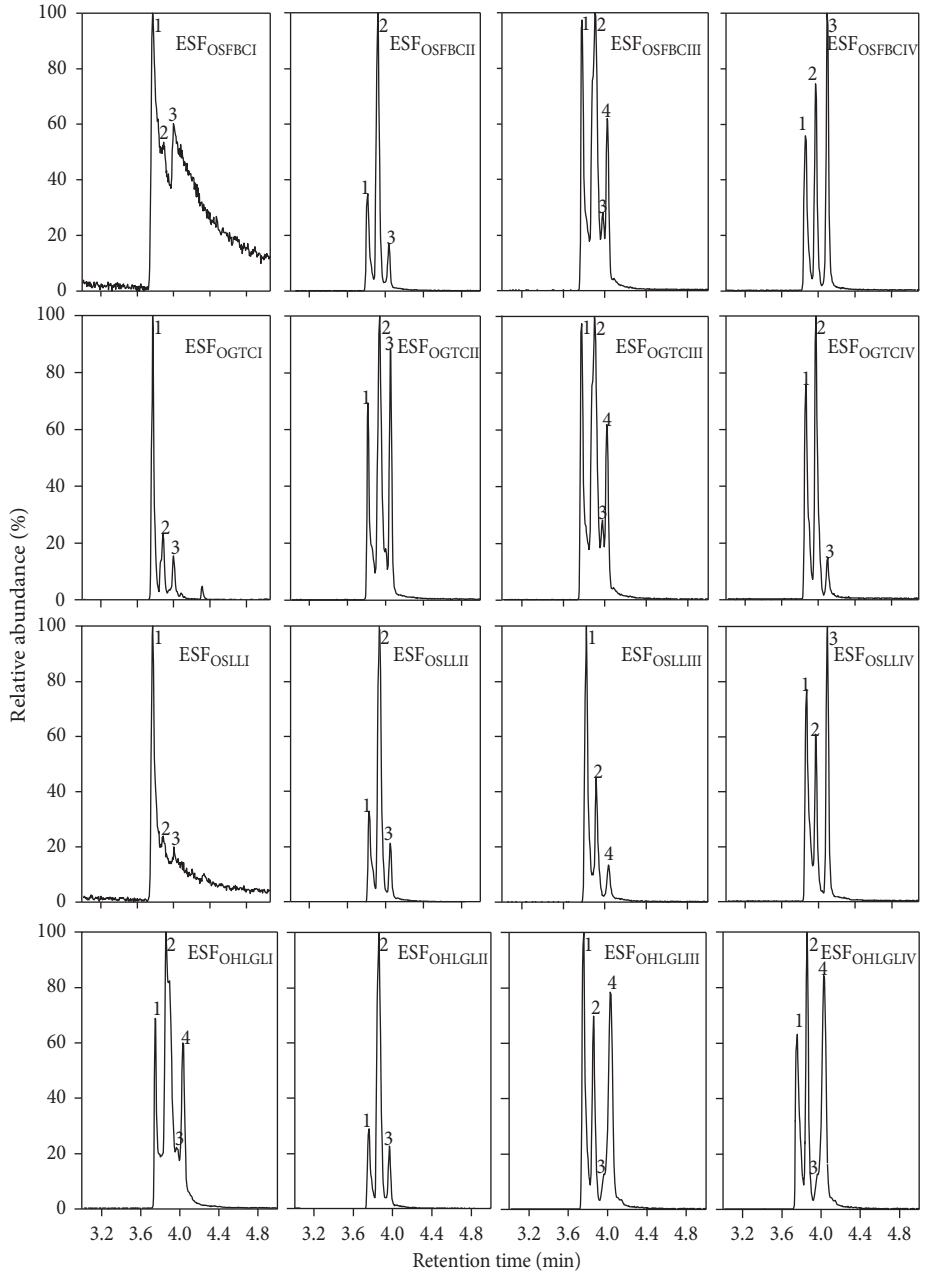

Figure 4: Water-soluble ether extract fraction analysis of oxidation coals.

According to the different species and number of OMs, coals with different coalification degrees are oxidized with different susceptibilities and can be converted into different species of OCOCs successfully. Furthermore, the second system (II) has the strongest oxidation resistance, and the first (I), third (III), and fourth (IV) systems have weaker oxidation resistance. In other words, the EYs of SFBC, GTC, and SLL in the second system are higher than those of the other three systems, and the numerical values of which are separately by 18%, 8.8%, and 37.4%. This study has proven that OMs in coals can be converted into stronger polar compounds if 0.1 g catalysts give that 12 hours of reaction time are available. Meanwhile, partly oxidized products may also be formed and dissolved in an aqueous solution, rarely leading to ESF. Compared with the open system, the isolated oxygen system involving only H_2O_2 OMs oxidation conversion laws is easier to analyze.

Finally, the weights of ESFs, ASFIs, and ASFIIs were considered (with SFBC as representative), in which the values of tube weight with dried extract and the weight of the plain tube are different. The results show that the value of WASFI is 0 and the weights of ESFs and ASFIIs are, respectively, 0.0756 and 0.1559 g in SFBC (ca. 2 g), indicating that the conversion rate of SFBC is 11.57% in the process.

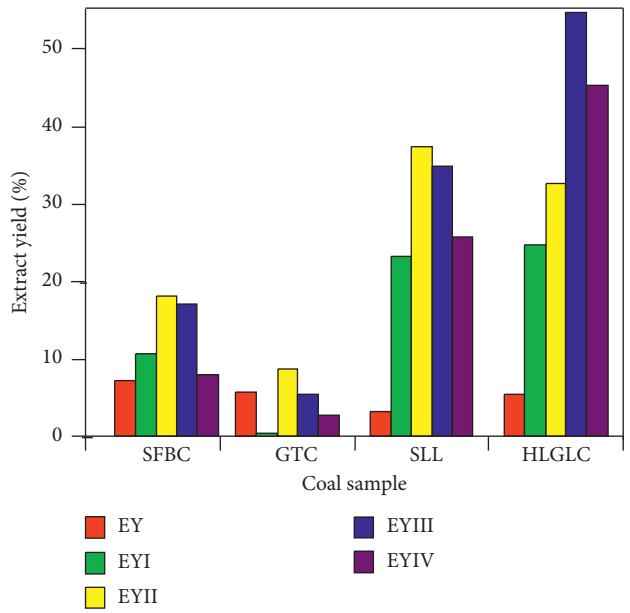

Figure 5: Extract yield of coals and oxidation coals.

4. Conclusions

In CSS, the process of PCO of OMs in coals can be oxidized and converted into many OCOCs via ring-opening and bond-breaking reactions through free radical substitution reaction and electrophilic reaction over SFC/TiO_2 under UV light illuminating the strong polar environment.

(1) OCOCs mainly include esters, ketones, aldehydes, and acids, and the final products are carbon dioxide and water. Acetic acid is the main generated intermediate species and is easy to dissolve in an aqueous solution. The number and species of products depend on the oxidation intensity and the polarity of the solution.

(2) Lignite can oxidize more easily than bituminite, which indicate that the OMs in the coal possibly have more active hydrogen molecules or bridge bond hydrogen as a result of the distribution in different regions with different formation environments and formation periods.

(3) The EY of coals can be improved in the process of PCO. The improvement facilitates the structure analysis and efficiency utilization of coal through the solution polarity and the dispersibility of OM enhancement, also including the decoloring of coal.

Nomenclature

PCO: Photocatalytic oxidation
CSS: Closed suspension system
FPs: Filtrate portions
FCs: Filter cakes
ESFs: Ether-soluble fractions
EIFs: Ether-insoluble fractions
ASFIs: Acetone-soluble fraction in coals
ASFIIs: Acetone-soluble fraction in oxidized coals
SPs: Solid portions
LPs: Liquid portions
SFBC: Shenfu bituminous coal
GTC: Geting coal
SLLC: Shengli lignite coal
HLGLC: Holingola coal
OSFBC: Oxidized Shenfu coal
OGTC: Oxidized Geting coal
OSLL: Oxidized Xilinhot coal
OHLGLC: Oxidized Holingola coal
TICs: Total ion chromatograms
RC: Relative content
OMs: Organic matters
ASF: Acetone-soluble fraction
ESF: Ether-soluble fraction
ASF_{SFBC}: Acetone-soluble fraction Shenfu coal
ASF_{GTC}: Acetone-soluble fraction Geting coal
ASF_{SLL}: Acetone-soluble fraction Shengli lignite
ASF_{HLGLC}: Acetone-soluble fraction Holingola coal
WESF: Weight of ether-soluble fraction
ASF_{OSFBCI}: Acetone-soluble fraction OSFBC-I
$ASF_{OSFBCII}$: Acetone-soluble fraction OSFBC-II
$ASF_{OSFBCIII}$: Acetone-soluble fraction OSFBC-III
$ASF_{OSFBCIV}$: Acetone-soluble fraction OSFBC-IV
ASF_{OGTCI}: Acetone-soluble fraction OGTC-I
ASF_{OGTCII}: Acetone-soluble fraction OGTC-II
$ASF_{OGTCIII}$: Acetone-soluble fraction OGTC-III
ASF_{OGTCIV}: Acetone-soluble fraction OGTC-IV
ASF_{OSLLI}: Acetone-soluble fraction OSLL-I
ASF_{OSLLII}: Acetone-soluble fraction OSLL-II
$ASF_{OSLLIII}$: Acetone-soluble fraction OSLL-III
ASF_{OSLLIV}: Acetone-soluble fraction OSLL-IV
$ASF_{OHLGLCI}$: Acetone-soluble fraction OHLGLC-I
$ASF_{OHLGLCII}$: Acetone-soluble fraction OHLGLC-II
$ASF_{OHLGLCIII}$: Acetone-soluble fraction OHLGLC-III
$ASF_{OHLGLCIV}$: Acetone-soluble fraction OHLGLC-IV
NAs: Normal alkanes
BAs: Branched alkanes
CAs: Carboxylic acids
NSAs: Nonsubstituted arenes
NCOCs: Nitrogen-containing compounds
OCOCs: Oxygen-containing organic compounds
$WEEF_{OSIIV}$: Water-soluble ether extract fraction of OSFBCI-IV
$WEEF_{OGIIV}$: Water-soluble ether extract fraction of OGTCI-IV
$WEEF_{OXIIV}$: Water-soluble ether extract fraction of OSLLI-IV
$WEEF_{OHIIV}$: Water-soluble ether extract fraction of OHLGLCI-IV
WSEEF: Water-soluble ether extract fraction
EY: Extract yield
EY0: Extract yield of crude coal
EYI: Extract yield of OSFBC
EYII: Extract yield of OGTC
EYIII: Extract yield of OSLL

EYIV: Extract yield of OHLGLC
WFCs: Weight of filter cakes
WASFI: Weight of coal extracted with acetone
WASFII: Weight of oxidized coal extracted with acetone.

Data Availability

The data used to support the findings of this study are available from the corresponding author upon request.

Additional Points

SFBC, GTC, SLL, and HLGLC were illuminated in four systems, respectively. Coals were oxidized in the isolated oxygen system. OCOCs mainly include esters, oxy-compounds, oxocompounds, and acids. Extraction of coals has been enhanced after photooxidation.

Conflicts of Interest

The authors declare that they have no conflicts of interest in this study.

Acknowledgments

This work was supported by the National Natural Science Foundation of China (Project 50974121), the Research Project Fund for the Xuzhou City (KC16SQ180), the Science and Technology Projects for the Ministry of Housing and Urban–Rural Development (2013-K6-12), and the Science and Technology Projects for the Jiangsu Construction Department (2016-ZD10) and sponsored by Qing Lan Project (2014) and the Natural Science Foundation of the Jiangsu Higher Education Institutions of China (17KJA610001).

Supplementary Materials

Figure SI1: total ion chromatograms of the ASF_{SFBC}, ASF_{OSFBCI}, and $ASF_{OSFBCIV}$. Figure SI2: total ion chromatograms of ASF_{GTC} and ASF_{OGTCI}. Figure SI3: total ion chromatograms of the ASF_{SLL}, ASF_{SLLI}, and ASF_{SLLIV}. Figure SI4: total ion chromatograms of the ASF_{HLGLC} and ASF_{HLGLCI}. Table SI1: comparison analysis of compounds detected in $WEEF_{OSFBC}$, $WEEF_{OGTC}$, $WEEF_{OSLL}$, and $WEEF_{OHLGLC}$. Table SI2: extraction efficiency analysis of photocatalytic oxidation coals. (*Supplementary Materials*)

References

[1] K. Miura, "Mild conversion of coal producing valuable chemicals," *Fuel Processing Technology*, vol. 62, no. 2-3, pp. 119–135, 2002.
[2] H. H. Schobert and C. Song, "Chemicals and materials from coal in the 21st century," *Fuel*, vol. 81, no. 1, pp. 15–32, 2002.
[3] R. Liotta, G. Brons, and J. Isaacs, "Oxidative weathering of Illinois No.6 coal," *Fuel*, vol. 62, no. 7, pp. 781–791, 1983.
[4] M. Italy, C. Hill, and D. A. Glasser, "A study of the low temperature oxidation of coal," *Fuel Processing Technology*, vol. 21, no. 2, pp. 81–97, 1989.
[5] Y. X. Li, B. Xue, N. Liu, and K. A. Pradeep, "Thermodynamics law of low temperature oxidation of low rank coal wet oxygen," *Coal Conversion*, vol. 30, pp. 1–5, 2007.
[6] Z. X. Liu, Z. C. Liu, Z. M. Zong, X. Y. Wei, J. Wang, and C. W. Lee, "GC/MS analysis of water-soluble products from the mild oxidation of longkou brown coal with H_2O_2," *Energy & Fuels*, vol. 17, no. 2, pp. 424–426, 2003.
[7] I. Takaaki, T. Hideyuki, K. Katsuki, and M. Shigeharu, "Structural changes of alcohol-solubilized yallourn coal in the hydrogenation over a Ru/Al_2O_3 catalyst," *Energy Fuels*, vol. 12, no. 3, pp. 503–511, 1998.
[8] Ü. Sevil, G. Zehra, and S. P. Yalcin, "Effects of coal oxidation on calorific value," *Energy Sources*, vol. 21, no. 3, pp. 269–273, 1999.
[9] Y. G. Huang, Z. M. Zong, Z. S. Yao et al., "Ruthenium ion-catalyzed oxidation of Shenfu coal and its residues," *Energy & Fuels*, vol. 22, no. 3, pp. 1799–1806, 2008.
[10] B. Chen, X. Y. Wei, Z. M. Zong, Z. S. Yang, Y. Qing, and C. Liu, "Difference in chemical composition of supercritical methanolysis products between two lignites," *Applied Energy*, vol. 88, no. 12, pp. 4570–4576, 2011.
[11] J. Liu, X. Y. Wei, Y. G. Wang et al., "Mild oxidation of Xiaolongtan lignite in aqueous hydrogen peroxide-acetic anhydride," *Fuel*, vol. 142, pp. 268–273, 2015.
[12] F. J. Liu, Z. M. Zong, J. Gui, X. N. Zhu, X. Y. Wei, and L. Bai, "Selective production and characterization of aromatic carboxylic acids from Xianfeng lignite-derived residue by mild oxidation in aqueous H_2O_2 solution," *Fuel Processing Technology*, vol. 181, pp. 91–96, 2018.
[13] J. H. Lv, X. Y. Wei, Y. Y. Zhang, and Z. M. Zong, "Mild oxidation of Yanshan petroleum coke with aqueous sodium hypochlorite," *Fuel*, vol. 226, pp. 658–664, 2018.
[14] Y. G. Wang, X. Y. Wei, H. L. Yan et al., "Mild oxidation of Jincheng No. 15 anthracite," *Journal of Fuel Chemistry and Technology*, vol. 41, no. 7, pp. 819–825, 2013.
[15] Z. S. Yao, X. Y. Wei, J. Lv et al., "Oxidation of Shenfu coal with RuO_4 and NaOCl," *Energy & Fuels*, vol. 24, no. 3, pp. 1801–1808, 2010.
[16] A. L. Faria, T. C. O. Mac Leod, and M. D. Assis, "Carbamazepine oxidation catalyzed by iron and manganese porphyrins supported on aminofunctionalized matrices," *Catalysis Today*, vol. 133-135, pp. 863–869, 2008.
[17] H. Takagi, T. Isoda, K. Kusakabe et al., "Structural changes in alcohol-solubilized coals by hydrogenation over a Ru/Al_2O_3 catalyst and effects on pyrolysis reactivities," in *The 6th Japan-Chinese Symposium on Coal Cl Chemistry Proceeding*, pp. 15–18, Zao, Miyagi, Japan, July 1998.
[18] K. Miura, K. Mae, H. Okutsu, and N.-A. Mizutani, "New oxidative degradation method for producing fatty acids in high yields and high selectivity from low-rank coals," *Energy & Fuels*, vol. 10, no. 6, pp. 1196–1201, 1996.
[19] K. Mae, H. Shindo, and K. Miura, "A new two-step oxidative degradation method for producing valuable chemicals from low rank coals under mild conditions," *Energy & Fuels*, vol. 15, no. 3, pp. 611–617, 2001.
[20] A. Fujishima and K. Honda, "Electrochemical photolysis of water at a semiconductor electrode," *Nature*, vol. 238, no. 5358, pp. 37-38, 1972.
[21] A. Fujishima and K. Honda, "Electrochemical evidence for the mechanism of the primary stage of photosynthesis," *Bulletin of the Chemical Society of Japan*, vol. 44, no. 4, pp. 1148–1150, 1971.
[22] M. R. Hoffmann, S. T. Martin, W. Choi, and D. W. Bahnemann, "Environmental applications of semiconductor photocatalysis," *Chemical Reviews*, vol. 95, no. 1, pp. 69–96, 1995.

[23] T. M. Scot, C. L. Morrison, and M. R. Hoffman, "Photochemical mechanism of size-quantized vanadium-doped TiO_2 particles," *The Journal of Physical Chemistry*, vol. 98, no. 51, pp. 13695–13764, 1994.

[24] R. Asahi, T. Morikawa, T. Ohwaki et al., "Visible-light photocatalysis in nitrogen-doped titanium oxides," *Science*, vol. 293, no. 5528, pp. 269–271, 2001.

[25] Y. M. Cho, W. Y. Choi, C. H. Lee, T. Hyeon, and H. I. Lee, "Visible light-induced degradation of carbon tetrachloride on dye-sensitized TiO_2," *Environmental Science & Technology*, vol. 35, no. 5, pp. 966–970, 2001.

[26] Z. J. Han, F. Qiu, R. Eisenberg, P. L. Holland, and T. D. Krauss, "Robust photogeneration of H_2 in water using semiconductor nanocrystals and a nickel catalyst," *Science*, vol. 338, no. 6112, pp. 1321–1324, 2012.

[27] W. Choi, A. Termin, and M. R. Hoffmann, "The role of metal ion dopants in quantum-sized TiO_2: correlation between photoreactivity and charge carrier recombination dynamics," *The Journal of Physical Chemistry*, vol. 98, no. 51, pp. 13669–13679, 1994.

[28] H. Chen, Z. M. Zong, J. W. Zhang et al., "Analysis of products from the oxidation of Heidaigou coal residue with H_2O_2 aqueous under mild condition," *Journal of China University of Mining & Technology*, vol. 37, pp. 347–354, 2008.

[29] Y. F. Jiang, K. S. Li, A. N. Zhou et al., "Photoactivated oxidization properties of Shenfu coal," *Coal Conversion*, vol. 27, pp. 83–86, 2004.

[30] M. Sun, A. N. Zhou, Y. T. Zhang et al., "Study on photo coupled thermo-oxidation of Shenfu coal," *Journal of China Society*, vol. 34, no. 9, pp. 1244–1249, 2009.

[31] M. Sun, A. N. Zhou, and Q. X. Yao, "Photocatalysis oxidating of coal in liquid phase," *Journal of China Society*, vol. 35, pp. 1553–1558, 2010.

[32] H. L. Gao, J. M. Gao, J. Zhang, Z. Zhu, G. Zhang, and Q. Liu, "Influence of carbon and yttrium co-doping on the photocatalytic activity of mixed phase TiO_2," *Chinese Journal of Catalysis*, vol. 38, no. 10, pp. 1688–1696, 2017.

[33] H. S. Xie, Z. M. Zong, Q. Wei et al., "Photocatalytic oxidation of Shenfu bituminous coal and Xilinhaote lignite with H_2O_2 over TiO_2," *Advanced Materials Research*, vol. 233-235, pp. 1684–1689, 2011.

[34] H. S. Xie, Z. M. Zong, T. Liu et al., "Photo-catalytic oxidation of Shenfu coal and Xilinhot lignite in heterogeneous hydration system," *Journal of China Coal Society*, vol. 36, no. 5, pp. 849–854, 2011.

[35] H. S. Xie, Z. M. Zong, S. H. Zhang et al., "Characterization of SFC-TiO_2 and application in DVR depolymerization," *Journal of China University of Mining & Technology*, vol. 40, no. 2, pp. 279–286, 2011.

[36] H. S. Xie, Z. M. Zong, S. H. Zhang et al., "Organic matters conversion law in heavy carbon resources under UV light illumination," *Journal of Wuhan University of Technology*, vol. 35, pp. 123–129, 2013.

[37] Z. Y. Yang and A. N. Zhou, "Study on catalytic photo-oxidation degradation of Shenfu coal by FITR," *Journal of China Coal Society*, vol. 30, pp. 759–764, 2005.